01 Aug 2006

Predicting TEM Cell Measurements from Near Field Scan Data

Haixiao Weng

Daryl G. Beetner
Missouri University of Science and Technology, daryl@mst.edu

Richard E. DuBroff

Recommended Citation

H. Weng et al., "Predicting TEM Cell Measurements from Near Field Scan Data," *Proceedings of the 2006 IEEE International Symposium on Electromagnetic Compatibility (2006, Portland, OR)*, Institute of Electrical and Electronics Engineers (IEEE), Aug 2006.
The definitive version is available at https://doi.org/10.1109/ISEMC.2006.1706371

Predicting TEM Cell Measurements from Near Field Scan Data

Haixiao Weng, Daryl G. Beetner, and Richard E. DuBroff
Electromagnetic Compatibility Laboratory
University of Missouri-Rolla
Rolla, MO 65409, USA
Email address: haixiao.weng@umr.edu

***Abstract*—A procedure is proposed for predicting TEM cell measurements from near field scans by modeling near-field scan data using equivalent sources. The first step in this procedure is to measure the tangential electric and magnetic fields over the circuit. Electric and magnetic fields are estimated from probe measurements by compensating for the characteristics of the probe. An equivalent magnetic and electric current model representing emissions is then generated from the compensated fields. These equivalent sources are used as an impressed source in an analytical formula or full wave simulation to predict measurements within the TEM cell. Experimental verification of the procedure using a microstrip trace and clock buffer show that values measured in the TEM cell and calculated from near field scan data agree within a few decibels from 1 MHz to 1 GHz.**

Keywords-TEM cell; near field measurement; equivalent source; modeling; electromagnetic emissions

I. Introduction

IEC standard 61967 defines methods to measure conducted and radiated electromagnetic disturbances from integrated circuits (ICs) [1][2]. In many cases, the potential for an IC to couple to nearby objects and drive emissions is measured using the TEM-cell method (Part 2 of IEC 61967). A special TEM cell board must be manufactured to make this measurement. Unfortunately, the manufacture of this board may not be practical in all cases. In these instances, it may be more desirable to predict the TEM cell measurement from other measurements that can be made with more general test setups.

IEC standard 61967-3, the surface scan method, is also used to describe emissions from integrated circuits. Previous research has shown correlations between the surface scan over an IC and TEM cell measurements [3]. These correlations, however, were based on experimental rather than theoretical methods and did not give a precise method to numerically predict the TEM cell measurement from the near-field scan.

In this paper, we develop a means to predict TEM cell measurements from near-field scan data using an equivalent-source representation of the near electric and magnetic fields over the IC surface [4]. The coupling to the TEM cell is predicted by measuring the near electric and magnetic fields over the device under test (DUT), compensating the measurements to account for probe characteristics, and generating an equivalent source model. The final step then consists of either modeling the source and nearby structures in a full wave simulation environment to predict the TEM cell measurement or predicting the measurement from an analytical approximation of the fields. One advantage of this technique is that it may easily be extended to analyze the performance of a variety of different structures (for example enclosures) before they are built.

The methods and theory behind our approach is presented in the following paper, along with an experimental demonstration of its capabilities. The paper is organized as follows. First, the analytical formulations for predicting TEM cell measurements from electric and magnetic near field measurements are presented. This method is then used to predict the TEM cell measurements from a microstrip trace and then a clock buffer chip. The paper finishes with a discussion of results.

II. Theory

A TEM cell (Fig. 1 and Fig. 2) measures the potential of an IC to cause radiated emissions by measuring the energy coupled from the chip and package through capacitive and inductive mechanisms to a metal plate – the septum – inside the cell. The TEM cell used in this paper is FCC-TEM-JM1. Its dimensions are 15.2 x 9.9 x 33.8 cm. A detailed cross-section of the cell is shown in Fig. 2. Its geometry approximates a rectangular 50-ohm transmission line. The first higher order mode of the cell is the TE_{01} mode with cutoff frequency $f_{c(01)} = 1\,GHz$ [2][5]. The cell is coupled at both ends to conventional coaxial connectors via tapered sections. If the cell is terminated with its characteristic impedance and it operates below the cutoff frequency of its upper modes, only a propagating TEM mode wave is generated [5].

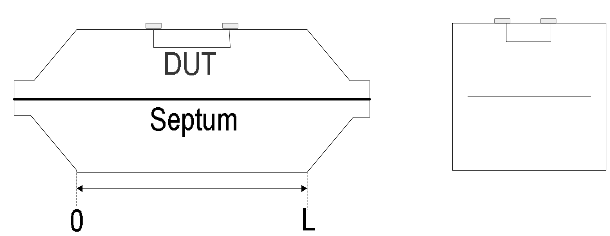

Figure 1. Cross sections of a TEM cell.

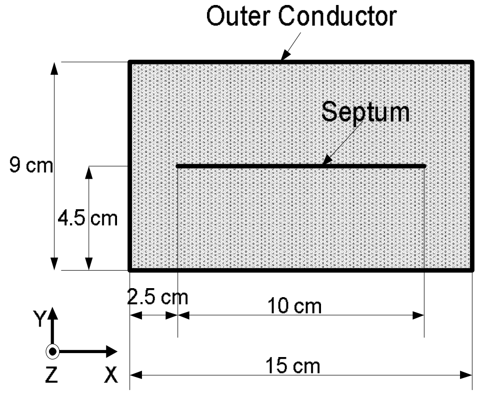

Figure 2. Detailed cross-section of the TEM cell.

If the excitation frequency is below the TE_{01} mode cutoff frequency, so that only the TEM mode is excited, then the voltage generated at the end of the TEM cell is given by the following equations [5][6][7]:

$$V_{TEM}^{+} = -\frac{Z_0}{2}\int_V \left(\vec{h}_{TEM}\cdot\vec{M} + \vec{e}_{TEM}\cdot\vec{J}\right)e^{j\beta_{TEM}Z}dv \quad , \qquad (1)$$
$$V_{TEM}^{-} = -\frac{Z_0}{2}\int_V \left(-\vec{h}_{TEM}\cdot\vec{M} + \vec{e}_{TEM}\cdot\vec{J}\right)e^{-j\beta_{TEM}Z}dv$$

where V_{TEM}^{+} and V_{TEM}^{-} represents the voltage measured at the two ports of the TEM cell, $\vec{J}$ and $\vec{M}$ are the electric and magnetic currents exciting the cell, Z_0 is the characteristic impedance of the TEM cell (taken as 50 Ω in this case), β_{TEM} is the field propagation constant, $\vec{e}_{TEM}$ is an electric vector transverse to the direction of propagation along the positive z axis (See Fig. 2), $\vec{h}_{TEM}$ is a magnetic vector transverse to the direction of propagation along the positive z axis, Sc is a surface in the x-y plane bounded by the septum and enclosure (shaded region in Fig. 2), and v is the volume enclosed by the TEM cell. Here, the terms $\vec{e}_{TEM}$ and $\vec{h}_{TEM}$ are used to represent the spatial distribution of the fields within the TEM cell by applying a unit amplitude incident wave at the port ($V^{+}=1$) and are not dependent on the device under test.

The values of $\vec{e}_{TEM}$ and $\vec{h}_{TEM}$ can be found using the integral equation method [7]. Alternatively, they can also be found by regarding the electric and magnetic fields as constant over the scan area. Since the scanning plane and the chip are very close to the bottom of the TEM cell relative to the height of the TEM cell, $\vec{e}_{TEM}$ and $\vec{h}_{TEM}$ are approximately unchanging in that region [5], so that:

$$\vec{e}_{TEM} = \frac{1}{4.5\ \text{cm}} = 22 \quad \text{V/m} \quad , \qquad (2)$$
$$\vec{h}_{TEM} = \frac{\vec{e}_{TEM}\times\hat{z}}{\eta} = \frac{22}{377} \quad A/\text{m}$$

Correlation of near field measurements with TEM cell measurements requires defining the tangential electric or magnetic fields on a surface surrounding the emissions source. According to IEC standard 61967-2, only the IC is allowed within the cell. Since all other circuitry and connections are located outside the cell on the other side of the test board, a near field scan is only required around the IC. To completely define the fields about the IC requires scanning five planar surfaces, as one surface is defined by the ground plane. If the scanning area is large compared to the height of the scan above the ground plane and the IC area, as is typically the case, then the contribution of fields on the side walls can be ignored and only the fields on the plane parallel to the IC must be measured.

Since the electric field associated with the TEM mode is normal to the septum, impressed electrical currents parallel with the septum can not excite any TEM modes (i.e. $\vec{e}_{TEM}\cdot\vec{J}_S = 0$ when $\vec{J}_S$ is defined in the plane parallel to the septum). The coupling between the circuit and the TEM cell can be expressed as

$$\begin{aligned} V_{TEM}^{+} &= -\frac{Z_0}{2}\int_V \left(\vec{h}_{TEM}\cdot\vec{M}_S + \vec{e}_{TEM}\cdot\vec{J}_S\right)e^{j\beta_{TEM}Z}dv \\ &= -\frac{Z_0}{2}\int_S \left(\vec{h}_{TEM}\cdot\vec{M}_S\right)e^{j\beta_{TEM}Z}ds \\ &= -\frac{Z_0}{2}\int_S \left(h_{TEM}M_{Sx}\right)e^{j\beta_{TEM}Z}ds \\ &= -\frac{Z_0}{2}\int_S \left(h_{TEM}E_{Sz}\right)e^{j\beta_{TEM}Z}ds \\ &= -\frac{550}{377}\int_S E_{Sz}e^{j\beta_{TEM}Z}ds \end{aligned} \qquad (3)$$

where $\vec{M}_s$ is the equivalent magnetic surface currents in the plane above the IC, $\vec{M}_s = -\hat{n}\times\vec{E}_s$, M_{Sx} is the component in the x direction, $\vec{J}_s$ is the equivalent electric surface current, $\vec{J}_s = \hat{n}\times\vec{H}_s$, E_{Sz} is the magnitude of the surface electric field in the z direction, and the integrals are performed over the surface or volume defined by the near field scan. Using this relationship, the TEM cell measurement can be approximated from the equivalent electric or magnetic current sources using (3), by performing the surface integral of the equivalent electric field E_{Sz}.

III. Prediction of TEM Cell Measurements From Near Field Measurements

To demonstrate the accuracy of our approach, near electric and magnetic fields were measured over a microstrip trace and a clock buffer and were used to predict TEM cell measurements.

A small dipole antenna and a small loop probe made from coaxial cables were used to measure the near tangential electric and magnetic fields over the device surface. The probes were calibrated and the measurement compensated using methods given in [4]. Since the compensation procedure is ill-posed for terms with high spatial frequency, a spatial wave number domain filter was added to filter out high spatial frequency noise in the wave number domain [11]. The influence of these terms on the TEM cell measurement is minimal since these terms dissipate very quickly.

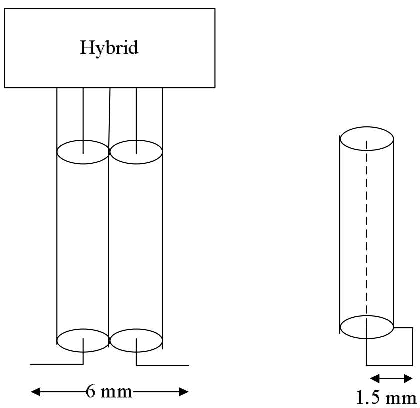

Figure 3. Probes used to measure electric and magnetic fields (to the left and right, respectively).

A. Measurement of a Microstrip Trace

The microstrip used to test our methods is shown in Fig. 4. The trace is 20 mm long by 2 mm wide and the circuit board is 100 mm along each edge. The trace was fed at one end through an SMA connector on the back side of the board and was terminated with a 50-ohm load at the other end.

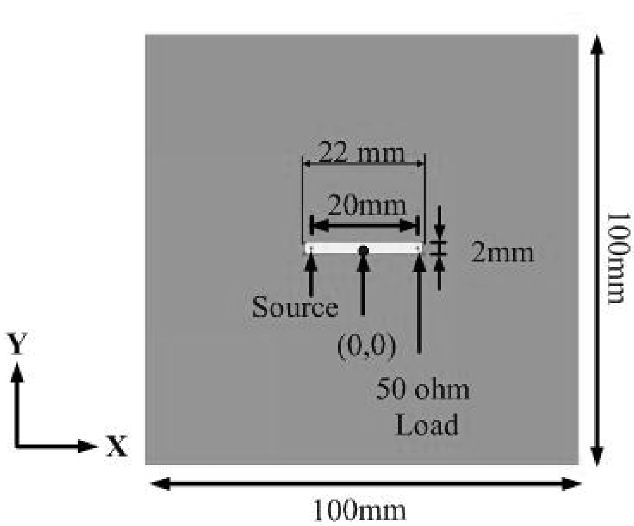

Figure 4. Front view of the measured microstrip structure.

The microstrip trace was scanned as shown in Fig. 5. The electric and magnetic fields were measured and calibrated over a plane 2.4-mm above the trace. Measurements were made over a 75 mm by 75 mm square area parallel to the microstrip trace. The center of the scan area and the center of the microstrip ground plane were set to coincide. The trace was driven by port 1 of a network analyzer and the field measured with port 2. Measurements were done at 50 MHz and at 100-MHz intervals from 100 MHz to 800 MHz. Fig. 6. shows the measured 200 MHz electric and magnetic fields over the microstrip trace after calibration and compensation.

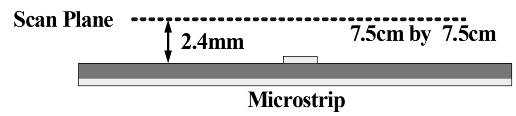

Figure 5. Definition of scan plane above microstrip.

TEM cell measurements for the microstrip trace were obtained experimentally, were predicted from a full-wave simulation of the trace and cell, and were predicted from the equivalent source representation of the near electric and magnetic fields measured over the trace using (3). Experimental measurements of TEM cell emissions were made as shown in Fig. 7. The trace was driven by port 1 of a network analyzer and measurements were made with port 2. Fig. 8 and Fig. 9 show the value of S_{21} for the microstrip trace coupled to the near and far end of the TEM cell as found experimentally, as calculated from a full wave simulation, and as predicted using the equivalent source model derived from near field scans. The experimental and predicted values match within a few decibels up to several hundred MHz.

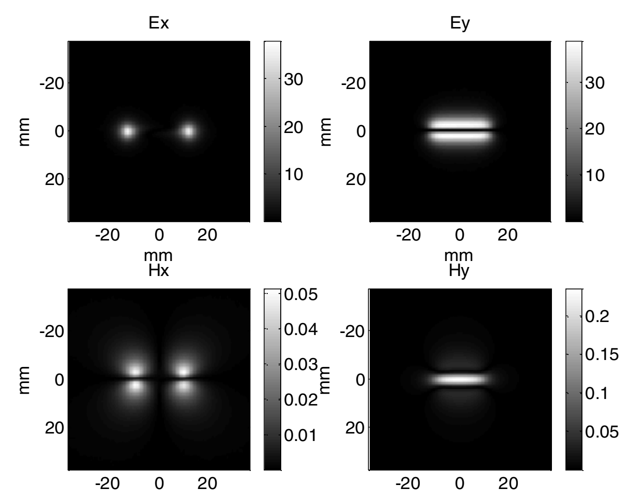

Figure 6. The electric and magnetic field at 200-MHz, 2.4 mm above the microstrip surface after compensation (1 volt source voltage assumed).

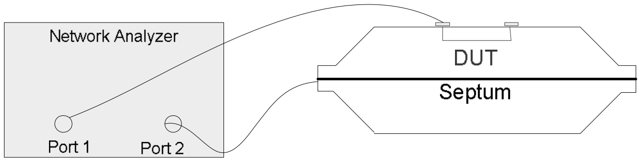

Figure 7. Measurement of near-end coupling.

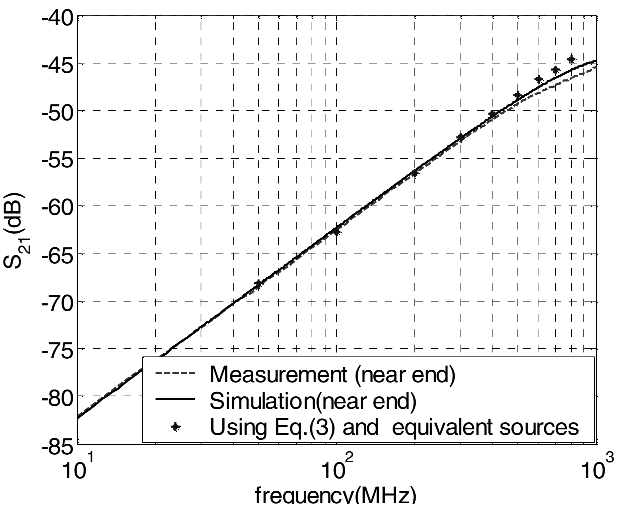

Figure 8. S_{21} as measured experimentally, as predicted from a full wave model, and as predicted by an equivalent source model (near end).

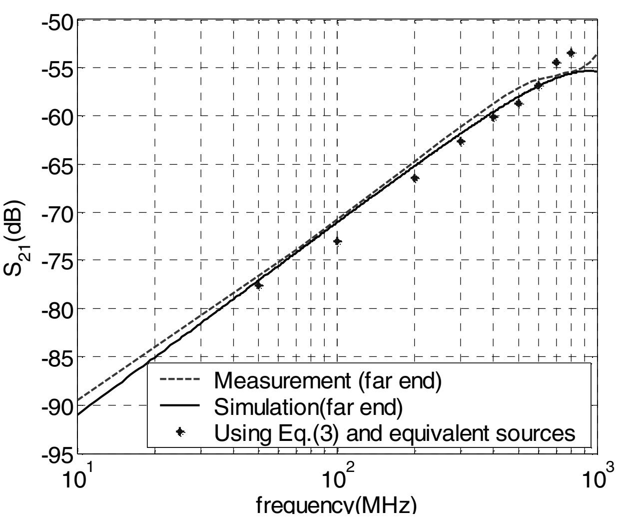

Figure 9. S_{21} as measured experimentally, as predicted from a full wave model, and as predicted by an equivalent source model (far end).

B. Measurement of a Clock Buffer

TEM cell measurements for a 1-to-10 clock driver (IDT74FCT807BT/CT) were also estimated from near field scans [12]. Fig. 10 shows a picture of the driver's lead frame. The lead frame was approximately 1.2 mm above a solid return plane. The chip was fed by a 100 MHz clock through an SMA connector on the back of the board connected to the 'IN' pin on the top left corner of the chip. All output pins except pins 11 and 18 were left floating. Pins 11 and 18 were terminated to the ground plane through 47 pF and 100 pF capacitor loads.

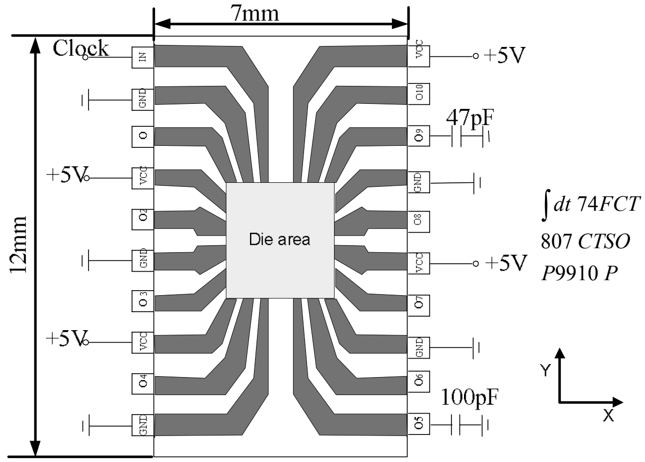

Figure 10. The clock buffer and its connections.

Near electric and magnetic fields were measured as shown in Fig. 11. The output of the probe was connected to a pre-amplifier with 25 dB gain using a 50-Ω coaxial cable. The characteristics of the amplifier and cable were calibrated using an HP8753d network analyzer. During scanning, measurements were made with a Tektronix TDS 520A oscilloscope. A dual-probe approach was used to synchronize the measurements made at different locations as described in [13], allowing an accurate measurement of phase. A second loop probe was placed over the chip surface and used to generate a trigger signal.

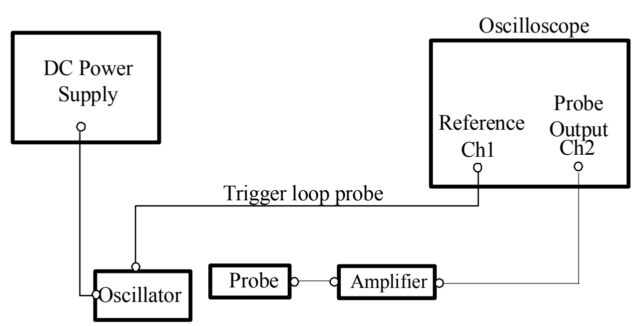

Figure 11. Measurement of near electric and magnetic field over chip surface.

The near tangential electric and magnetic fields in a plane just over the chip surface were measured and compensated as before. The circuit was scanned over a 6 cm by 6 cm area at 91 by 91 sample points. The measured time domain signal was transformed into the frequency domain using the fast Fourier transform. Fig. 12 shows the compensated electric field measured at 100 MHz. Our measurements also found significant field components at harmonics of 100 MHz up to 1 GHz.

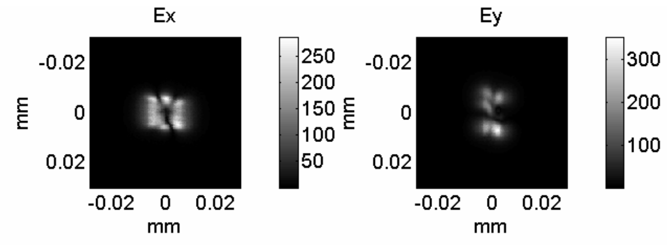

Figure 12. The electric field above the clock buffer at 100-MHz after compensation.

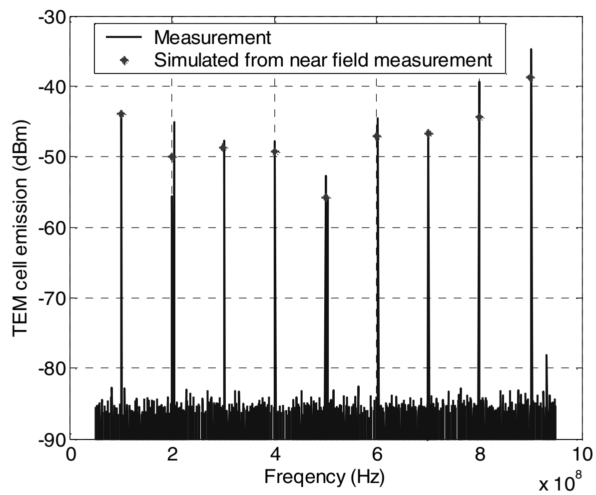

Figure 13. TEM cell emissions from a clock buffer IC as measured and as predicted by an equivalent source model.

TEM cell measurements from the clock driver were predicted by substituting the compensated field into (8). TEM cell emissions were predicted and measured with the IC oriented in four different directions inside the TEM cell (0º, 90º, 180º, and 270º). The maximum TEM cell output for these four directions was recorded and plotted in Fig. 13 (the 25 dB amplifier was taken into account in both measurement and prediction). The measurement and simulation match within 6 dB up to approximately 1 GHz.

The difference between the measurement and simulation seen here may be caused by the inherently ill-posed nature of the compensation problem [11]. The tangential electric field at $k_x = k_z = 0$ in the wave number domain is mainly due to inductive coupling. It is difficult to correctly compensate this plane wave contribution, because its contribution to the overall electric field is very small compared to the contribution of other components (i.e. when $k_z \neq 0$). That is, it is difficult to accurately measure the small $k_x = k_z = 0$ contribution in the presence of other, much larger, contributions. Errors in the compensated electric field at $k_x = k_z = 0$ have a relatively large effect on the TEM cell measurement, however, since the contribution of this component to the TEM cell measurement is roughly equivalent to the contribution of plane waves with $k_z \neq 0$. Thus, difficulties in accurately compensating the electric field may manifest themselves as errors in the calculated TEM cell measurement.

IV. Discussion and Conclusions

A procedure for predicting TEM cell measurements from near-field scan data using an equivalent source model was presented in this paper. Experiments performed on a microstrip trace and a clock buffer show that the predicted and measured TEM cell emissions agree within 6 dB up to several hundred MHz. Mismatch at higher frequencies may be caused by non-TEM modes excited in the TEM cell or by errors intrinsic to the compensation procedure.

References

[1] IEC 61967-2 "Integrated circuits - Measurement of electromagnetic emissions, 150 kHz to 1 GHz - Part 2: Measurement of radiated emissions, TEM-cell method"

[2] IEC 61967-3 "Integrated circuits - Measurement of electromagnetic emissions, 150 kHz to 1 GHz - Part 3: Measurement of radiated emissions, Surface scan method "

[3] B. Deutschmann, H. Pitsch, G. Langer, "Near field measurements to predict the electromagnetic emission of integrated circuits", 5th International Workshop on Electromagnetic Compatibility of Integrated Circuits, November, 2005, Munich, Germany.

[4] J. Shi, "Near-field measurement and analysis procedures for characterizing electromagnetic interference", dissertation presented to the faculty of the gradate school of Missouri – Rolla for degree of Ph. D, University of Missouri – Rolla, Feb. 2005.

[5] F. Fiori, F. Musolino, "Measurement of integrated circuit conducted emission by using a transverse electromagnetic (TEM) cell," IEEE Trans. on Electromagnetic Compatibility, vol. 43, no. 4, pp. 622-628, Nov. 2001.

[6] F. Fiori, F. Musolino and V. Pozzolo, "Weakness of the TEM cell method in evaluating IC radiated emissions," IEEE International Symposium on Electromagnetic Compatibility, vol. 1, Aug. 2001, pp. 135 – 138.

[7] D. M. Pozar, *Microwave engineering*, chapter 4: Micowave network analysis, *Engineering*, 2nd ed. New York:Wiley, 1998.

[8] R. J. Spiegel, W. T. Joines, C. F. Blackman, and A.W. Wood, "A method for calculating electric and magnetic fields in TEM cell at ELF", IEEE Trans. Electromagn. Compat., vol. EMC-29, pp. 265-272, Nov. 1987.

[9] G. S. Smith, *An Introduction to Classical Electromagnetic Radiation. Cambridge*, United Kingdom: Cambridge University Press, 1997.

[10] P.C. Clemmow, *The Plane Wave Spectrum Representation of Electromagnetic Fields*. Piscataway, NJ: IEEE Press, 1996.

[11] Adam Tankielun, Bertrand Vrignon, Uwe Keller, Werner John, Etienne Sicard, Heyno Garbe "Complex Deconvolution for Correction of Near-Field Measurements Applied to LSI Chip", proceedings of the 2nd International Conference on Electromagnetic Near-Field Characterization & Imaging (ICONIC 2005), ISBN 84-95999-72-2, pp 261-266, Barcelona, June 2005

[12] 74FCT807T Data Sheet, Integrated Device Technology, Inc., December 2000

[13] T. Stadtler, L. Eifler, J. L. ter Haseborg, "Double probe near field scanner, a new device for measurements in time domain", in Proc. 2003 IEEE Symp. Electromagnetic Compatibility, Boston, MA, pp. 86-90, Aug.18-22, 2003.